Eur. Phys. J. Appl. Phys. **35**, 173–176 (2006)
DOI: 10.1051/epjap:2006085

THE EUROPEAN PHYSICAL JOURNAL APPLIED PHYSICS

Anomalous photovoltaic effect in $La_{0.8}Sr_{0.2}MnO_3$ films grown on $SrTiO_3$ (001) substrates by laser molecular beam epitaxy

Kun Zhao[1,2,3,a], Hui-bin Lu[2], Meng He[2], Yan-hong Huang[2], Kui-juan Jin[2], Zheng-hao Chen[2], Yue-liang Zhou[2], Guo-zhen Yang[2], and Xiu-liang Ma[4]

[1] Department of Mathematics and Physics, China University of Petroleum, Beijing 102249, P.R. China
[2] Beijing National Laboratory for Condensed Matter Physics, Institute of Physics, Chinese Academy of Sciences, Beijing 100080, P.R. China
[3] International Center for Materials Physics, Chinese Academy of Sciences, Shenyang 110016, P.R. China
[4] Shenyang National Laboratory for Materials Science, Institute of Metal Research, Chinese Academy of Sciences, Shenyang 110016, P.R. China

Received: 24 September 2005 / Received in final form: 24 March 2006 / Accepted: 19 May 2006
Published online: 13 July 2006 –

Abstract. Transient laser-induced anomalous photovoltaic effect has been studied in $La_{0.8}Sr_{0.2}MnO_3$ films grown on the $SrTiO_3$ (001) substrates by laser molecular beam epitaxy. It is demonstrated that the signal polarity is reversed when the films are irradiated through the substrate rather than at the air/film interface. The microstructures in these films are clarified in terms of the oriented microdomains with their (101) plane parallel to the substrate surface, suggesting off-diagonal Seebeck effect plays an important role for our observation. From the results, we obtain the anisotropy of the thermoelectric power $\Delta S = S_{ab} - S_c = 0.3\ \mu$V/K, where S_{ab} and S_c are the ab-plane and c-axis Seebeck coefficients.

PACS. 72.40.+w Photoconduction and photovoltaic effects – 78.20.-e Optical properties of bulk materials and thin films

1 Introduction

The perovskite oxides have been investigated because of their interesting properties, including ferromagnetism, antiferromagnetism, metal-insulator transition, high T_C superconductivity, colossal magnetoresistance (CMR), optical properties and so on, depending on the carrier concentration due to strong coupling among the spin, charge, and orbital degrees of freedom [1–6]. During the past few years there has been active study of the photoresponse of the manganite thin films. Technological interest has centered on bolometers [7,8], while more basic issues have involved quasi-particle generation and carrier relaxation times [9–11].

Ultrafast photovoltaic effect has been observed in manganite oxide $La_{0.67}Ca_{0.33}MnO_3$ (LCMO) films under the irradiation of a laser pulse of 25 ps duration, and the rise time and full width at half-maximum (FWHM) are ∼300 ps and ∼700 ps, respectively [12]. It is noted that no photovoltage has been found when the photon energy is larger than the band gap of LCMO ($1 \sim 1.3$ eV) [12], demonstrating the production of the photon induced carriers plays a crucial role in the photovoltaic process.

Off-diagonal thermoelectricity, which may only occur in low symmetry environments, has been suggested to the laser-induced photovoltage (LIPV) in LCMO films on vicinal cut $SrTiO_3$ (STO) substrates [13]. Heating the film by the absorption of radiation establishes a temperature gradient ∇T perpendicular to the film surface. Due to the Seebeck effect a thermoelectric field

$$\mathsf{E} = \mathsf{S} \cdot \nabla T \tag{1}$$

is generated, where S is the Seebeck tensor and is of the form,

$$\mathsf{S} = \begin{pmatrix} S_{ab}\cos^2\alpha + S_c \sin^2\alpha & 0 & (S_{ab} - S_c)\sin(2\alpha)/2 \\ 0 & S_{ab} & 0 \\ (S_{ab} - S_c)\sin(2\alpha)/2 & 0 & S_{ab}\sin^2\alpha + S_c\cos^2\alpha \end{pmatrix}. \tag{2}$$

Here S_{ab} and S_c are the Seebeck coefficients of the crystalline ab-plane and along c-axis, respectively, and α is the tilt angle between the surface and surface normal n. The off-diagonal element give rise to an electrical field perpendicular to the temperature gradient leading to a LIPV

$$U = \frac{l}{2d}(S_{ab} - S_c)\sin(2\alpha)\Delta T, \tag{3}$$

[a] e-mail: ainiphoto@163.com

where ΔT is the temperature difference between film surface and film bottom, l the diameter of the irradiated spot, d the film thickness.

Based on the above observations, it is reasonable to propose the LIPV in manganite oxide films on tilted substrates as a combination of photoelectron and Seebeck processes.

Microstructure is of great importance for understanding the interplay of structure, electronic transport, and light. Small angles between surface normal and c-axis, due to not precisely cut substrates or the film deposition process, have been reported early [14]. From the viewpoint of crystallography, three structural polymorphs were identified for $La_{1-x}Sr_xMnO_{3+\delta}$ [15], namely rhombohedral ($R\bar{3}c$), orthorhombic ($Pnma$), and monoclinic ($P2_1/c$). All these phases have a slightly deformed perovskite structure owing to the distortion of the MnO_6 octahedra. Our previous work have shown that microstructural characteristics in $La_{0.8}Sr_{0.2}MnO_3$ (LSMO) films are domain-oriented from the interface between the film and the STO (001) substrate [16]. These domains run through the thickness of the film and form a columnar structure. The (101) plane of each domain is parallel to the substrate surface, and the boundaries are 45° away from the interface normal [001]. These facts indicate that a photovoltaic signal can be detected in manganite oxide films on untilted substrates based on the above discussion.

In this paper, our focus is the LIPV generated in LSMO films on STO (001) substrates at room temperature. It is found that if a pulsed laser with an energy gap larger than that of LSMO irradiated the film between two electrical contacts, a transient potential difference was induced across the film. It is emphasized that the polarity of the signal was reversed if the film was irradiated through the substrate rather than the film, since the microstructures in the whole film are clarified in terms of the oriented microdomains with (101) planes parallel to the substrate surface.

2 Experimental technique

LSMO films of about 500 nm thickness were epitaxially grown on STO (001) substrates by computer-controlled laser molecular beam epitaxy (laser MBE) [17]. An in situ reflection high-energy electron diffraction (RHEED) system and charge coupled device (CCD) camera were used to monitor the growth process of the LSMO thin films. The base pressure of the epitaxy chamber was 1×10^{-8} Pa. The substrates were heated at 630 °C under an oxygen pressure of 2×10^{-4} Pa. The output of a Lambda Physik LEXTRA 200 excimer laser (308 nm, 20 ns, 2 Hz) was used as the laser source with an energy density of about 1 J/cm^2. The deposition rate was about 0.01 nm/pulse.

A JEOL 2010 transmission electron microscope (TEM) with a point resolution of 0.194 nm was used for the electron diffraction analysis and atomic imaging. For the photovoltaic measurement, two In electrodes separate from 6 mm were placed on the surface of the LSMO films along the [100] direction of the STO substrate, and were always kept in the dark to prevent the generation of any electrical contact photovoltaic effect. The irradiation area is 3×6 mm^2, and the signal was monitored with a sampling oscilloscope (500 MHz bandwidth) terminated into 1 MΩ at ambient temperature.

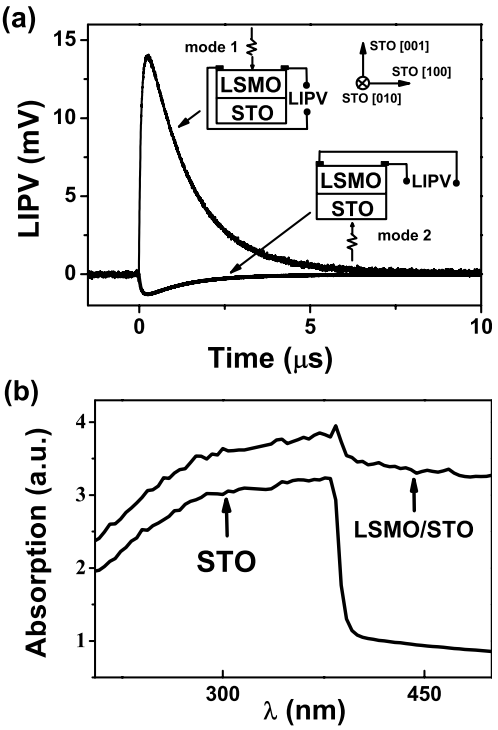

Fig. 1. (a) LIPV of LSMO (500 nm)/STO sample irradiated by a 355 nm laser pulse through the LSMO film side (mode 1) and STO substrate side (mode 2). (b) The absorption spectrum of STO substrate and LSMO (500 nm)/STO.

3 Results and discussion

Figure 1a shows typical photovoltaic pulses as a function of time for LSMO (500 nm)/STO together with the orientation of the laser beam, the third harmonic (355 nm) of an actively-passively mode-locked Nd:YAG laser with a duration of 25 ps and an energy density of 0.05 mJ/mm^2, with respect to the sample. Irradiating the film directly with the laser beam leads to a signal pulse of 14 mV, and the sensitivity of the LIPV over the energy of laser pulse is ∼16 mV/mJ. The response has a 10–90% rise time of 120 ns, a 10–90% fall time of 3 μs, and a full width at half maximum (FWHM) of 1.25 μs.

Especially, the signal polarity is reversed and the LIPV (∼1.5 mV) is 10 times lower when the LSMO film is irradiated through the STO substrate (mode 2) rather than at the air/LSMO interface (mode 1), the side to which the leads are attached. As presented in Figure 1b, STO single crystal exhibits a sharp absorption edge at 388 nm in agreement with its band gap of 3.2 eV and photocarriers can be generated under ultraviolet light with a wavelength of 355 nm. However, the substrate thickness

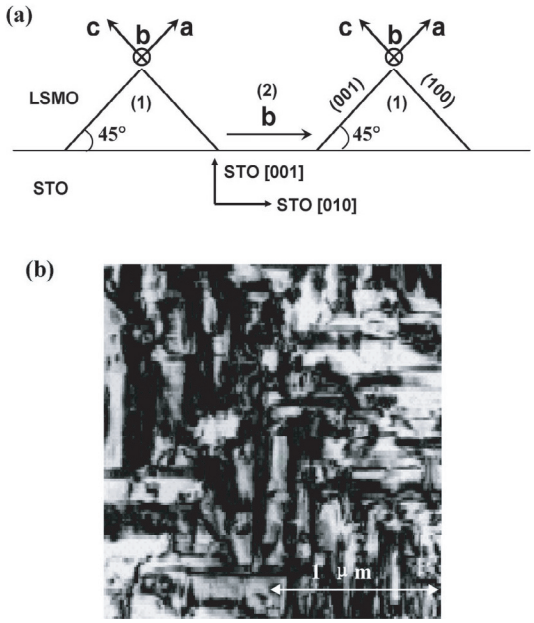

Fig. 2. (a) Schematic illustrations showing the orientations of the microdomains, marked with (1) and (2), at the interface of LSMO/STO. (b) A low-magnification plan-view image showing the domain distributions.

(0.5 mm) is much longer than the diffusion length of the photo-generated carriers in the STO side. In addition, due to strong absorption in STO substrate, few photons can inject into the LSMO layer and result in a small LIPV for mode 2.

Cross-section high-resolution image obtained at the interface of LSMO and STO shows that the film is epitaxially grown on the STO substrate [16]. Figure 2a illustrates the schematic drawing of the microdomains at the interface of LSMO/STO. The (101) planes in the domains are parallel to the substrate surface; the domains are at 90° to each other about the (101)-plane normal rotation, and the boundaries cross with each other at the interface. In order to obtain an overview of the oriented domain structures in LSMO films, a plan-view specimen was prepared. The low-magnification bright-field image shows that the domains form a rectangular cross-grid pattern, and the ratio of length to width is about 5 for each domain (Fig. 2b). All of these facts suggest an off-diagonal element,

$$S_{xz} = \frac{1}{2}(S_{ab} - S_c)\sin(2\alpha) = \frac{1}{2}(S_{ab} - S_c), \alpha = 45°, \quad (4)$$

is not equal to zero, which gives rise to an electric field along STO [100] direction perpendicular to the temperature gradient ∇T, resulting in a directional movement of the none-equilibrium photon-generated carriers in LSMO film under an irradiation of a short laser pulse and leading to a lateral voltage. This inversion of the signal which occurs when the direction of irradiation is reversed can be considered to be due to reversal of the ∇T in the thickness direction based in equation (1).

The LIPV effect of LSMO films were further investigated using a 1064 nm Nd:YAG laser, which is transparent for STO substrate, following the set-up in Figure 1. As shown in Figure 3, the signals generated by different irradiations are reverse. For mode 2, at 0.7 μs after completion of the laser pulse, the polarity of the signal changes and is the same as irradiating the free surface of the film. This observation proves the interpretation that the LIPV is caused by a temperature gradient normal to the film. As the heat flow from the film to the substrate is larger than from the free film surface to the ambient air, the temperature gradient in the freely cooling film gets reversed and, therefore, the LIPV changes sign.

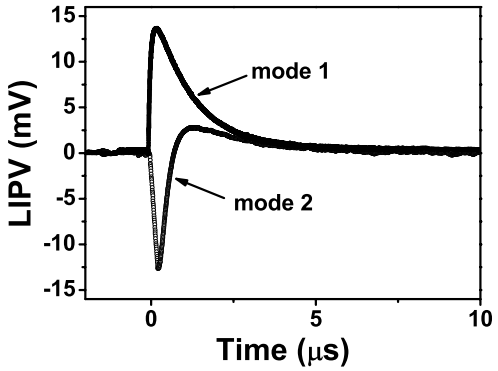

Fig. 3. The LIPV of LSMO film in response to 1064 nm pulsed laser for different geometries, mode 1 and mode 2.

From the heat flow equation

$$Q = \kappa \nabla T \approx \frac{E_{laser}}{\tau}, \quad (5)$$

the temperature gradient ∇T can be estimated. Here Q is the heat current density, τ response time, κ the surface-normal heat conductivity, E_{laser} the absorbed 1064 nm laser energy density and assumed as 0.05 mJ/mm^2 since LSMO films were found to have high absorption coefficient over a broad wavelength range. Thus,

$$U = \frac{l}{2}\frac{\sin(2\alpha)}{2}\frac{E_{laser}}{\kappa\tau}(S_{ab} - S_c) = \frac{lE_{laser}(S_{ab} - S_c)}{4\kappa\tau}, \quad (6)$$

at $\alpha = 45°$, where the factor 1/2 is due to the oriented domains with the b-axis parallel to STO [100] which do not make a contribution to the LIPV. Therefore we obtain $S_{ab} - S_c = 0.3$ μV/K, inserting $U = 12$ mV, $l = 6$ mm, $\tau = 1.25$ μs, and $\kappa = 1.5$ W/mK [18].

4 Conclusion

In conclusion, the anomalous photovoltaic effect have been investigated in LSMO films. The LIPV polarity is reversed when the films are irradiated through the substrate rather than directly by a laser pulse, which can be resulted from the off-diagonal Seebeck effect due to the oriented microdomains with the (101) planes perpendicular to STO [001] and at 90° to each other about the (101)-plane normal rotation.

This work has been supported by National Natural Science Foundation of China (Grant Nos. 10334070 and 60576015) and the National Key Basic Research and Development Program of China (Grant No. 2004CB619004).

References

1. C. Zener, Phys. Rev. **82**, 403 (1951)
2. K. Chahara, T. Ohno, M. Kasai, Y. Kozono, Appl. Phys. Lett. **63**, 1990 (1993)
3. R.V. Helmolt, J. Wecker, R. Holzapfel, L. Schultz, K. Samwer, Phys. Rev. Lett. **71**, 2331 (1993)
4. J.B. Barner, C.T. Rogers, A. Inam, R. Ramesh, S. Bersey, Appl. Phys. Lett. **59**, 742 (1991)
5. A. Lisauskas, S.I. Khartsev, A. Grishin, Appl. Phys. Lett. **77**, 756 (2000)
6. K. Zhao, Y.H. Huang, Q.L. Zhou, K.-J. Jin, H.B. Lu, M. He, B.L. Cheng, Y.L. Zhou, Z.H. Chen, G.Z. Yang, Appl. Phys. Lett. **86**, 221917 (2005); H.B. Lu, K.-J. Jin, Y.H. Huang, M. He, K. Zhao, B.L. Cheng, Z.H. Chen, Y.L. Zhou, S.Y. Dai, G.Z. Yang, Appl. Phys. Lett. **86**, 241915 (2005); K.-J. Jin, H.B. Lu, Q.L. Zhou, K. Zhao, B.L. Cheng, Z.H. Chen, Y.L. Zhou, G.Z. Yang, Phys. Rev. B **71**, 184428 (2005); K. Zhao, L. Zhang, H. Li, H.K. Wong, J. Appl. Phys. **95**, 7363 (2004); K. Zhao, L. Zhang, H.K. Wong, Thin Solid Films **471**, 287 (2005); K. Zhao, Y.H. Huang, J.F. Feng, L. Zhang, H.K. Wong, Physica C **418**, 138 (2005); K. Zhao, H.K. Wong, Physica C **403**, 119 (2004); K. Zhao, H.K. Wong, Physica B **349**, 238 (2004); K. Zhao, L.Z. Zhou, C.H. Leung, C.F. Yeung, C.K. Fung, H.K. Wong, J. Cryst. Growth **237/239**, 608 (2002)
7. M. Rajeswai, C.H. Chen, A. Goyal, C. Kwon, M.C. Robson, R. Ramesh, T. Venkatesan, S. Lakeou, Appl. Phys. Lett. **68**, 3555 (1996)
8. Y.M. Nikolaenko, I.S. Maksimov, A. Goyal, Y.V. Medevedev, A.N. Ulyanov, A.M. Grishin, Acta Phys. Pol. A **97**, 991 (2000)
9. Y.G. Zhao, J.J. Li, R. Shreekala, H.D. Drew, C.L. Chen, W.L. Cao, C.H. Lee, Phys. Rev. Lett. **81**, 1310 (1998)
10. R.D. Averitt, A.I. Lobad, C. Kwon, S.A. Trugman, V.K. Thorsmlle, A.J. Taylor, Phys. Rev. Lett. **87**, 017401 (2001)
11. R.L. Zhang, J.M. Dai, W.H. Song, Y.Q. Ma, J. Yang, J.J. Du, Y.P. Sun, J. Phys.-Condens. Matter **16**, 2245 (2004)
12. K. Zhao, Y.H. Huang, H.B. Lu, M. He, K.-J. Jin, Z.H. Chen, Y.L. Zhou, B.L. Cheng, S.Y. Dai, G.Z. Yang, Chinese Phys. **14**, 420 (2005)
13. H.-U. Habermeier, X.H. Li, P.X. Zhang, B. Leibold, Solid State Commun. **110**, 473 (1999)
14. J.D. Budai, M.F. Chisholm, R. Feenstra, D.H. Lowndes, D.P. Norton, L.A. Boatner, D.K. Christen, Appl. Phys. Lett. **58**, 2174 (1991)
15. J.F. Mitchell, D.N. Argyriou, C.D. Potter, D.G. Hinks, J.D. Jorgensen, S.D. Bader, Phys. Rev. B **54**, 6172 (1996)
16. X.L. Ma, Y.L. Zhu, X.M. Meng, H.B. Lu, F. Chen, Z.H. Chen, G.Z. Yang, Z. Zhang, Philos. Mag. A **82**, 1331 (2002)
17. H.B. Lu, N. Wang, W.Z. Chen, F. Chen, T. Zhao, H.Y. Peng, S.T. Lee, G.Z. Yang, J. Cryst. Growth **212**, 173 (2000); G.Z. Yang, H.B. Lu, H.S. Wang, D.F. Cui, H.Q. Yang, H. Wang, Y.L. Zhou, Z.H. Chen, Chinese Phys. Lett. **14**, 478 (1997)
18. B.X. Chen, A.G. Rojo, C. Uher, H.L. Ju, R.L. Greene, Phys. Rev. B **55**, 15471 (1997)